Basal conditions beneath enhanced-flow tributaries of Slessor Glacier, East Antarctica

D.M. RIPPIN,[1] J.L. BAMBER,[2] M.J. SIEGERT,[2*] D.G. VAUGHAN,[3] H.F.J. CORR[3]

[1]*Department of Geography, University of Hull, Cottingham Road, Hull HU6 7RX, UK*
E-mail: D.Rippin@hull.ac.uk
[2]*Bristol Glaciology Centre, School of Geographical Sciences, University of Bristol, University Road, Bristol BS8 1SS, UK*
[3]*British Antarctic Survey, Natural Environment Research Council, Madingley Road, Cambridge CB3 0ET, UK*

ABSTRACT. Radio-echo sounding data are used to investigate bed roughness beneath the three enhanced-flow tributaries of Slessor Glacier, East Antarctica. Slow-moving inter-tributary areas are found to have rough beds, while the bed of the northernmost tributary is relatively smooth. A reconstruction of potential subglacial drainage routing indicates that water would be routed down this tributary, and investigations of basal topography following isostatic recovery reveal that the bed would have been below sea level in preglacial times, so marine sediments may have accumulated here. Together, these factors are further support for the dominance of basal motion in this tributary, reported elsewhere. Conversely, although the other two Slessor tributaries may have water routed beneath them, they would not have been below sea level before the growth of the ice sheet, so cannot be underlain by marine sediments. They are also found to be rough, and, within the range of uncertainties, it is likely that basal motion does not play a major role in the flow of these tributaries. Perhaps the most interesting area, however, is a deep trough where flow rates are currently low but the bed is as smooth as the northern Slessor trough. It is proposed that, although ice deformation currently dominates in this trough, basal motion may have occurred in the past, when the ice was thicker.

INTRODUCTION

It is now accepted that tributaries of enhanced flow are widespread throughout both East and West Antarctica (Joughin and others, 1999; Bamber and others, 2000). Rather than there being an abrupt transition between streaming and inland flow (Alley and Whillans, 1991), tributaries represent a zone of gradual transition between these two flow regimes, in which flow occurs by some intermediate combination of internal deformation and basal motion (Joughin and others, 1999). The widespread existence of these tributaries within ice-sheet interiors has far-reaching implications for understanding ice-sheet flow and stability, which in turn is crucial for improving estimates of present-day and possible future changes in mass balance. As a consequence, it is important to better understand the mechanisms which control tributary flow.

An airborne radio-echo sounding (RES) campaign carried out in the upper reaches of the Slessor Glacier complex, in Coats Land, East Antarctica, has revealed that tributaries of enhanced flow lie within well-defined basal troughs, and are separated from each other by bed highs. As a consequence of these confining troughs, the large-scale location of these tributaries appears to be relatively stable. A numerical-modelling study indicates, however, that the contribution of basal motion to tributary flow can vary between tributaries, i.e. flow in the central and most southerly of the tributaries of Slessor Glacier can virtually all be explained by ice deformation (with basal motion, within the range of uncertainties, playing a very minor role), while flow in the northernmost tributary, under a similar glaciological setting, is largely due to basal motion (Rippin and others, 2003a).

We propose that variations in roughness may be responsible for this difference, because of the fundamental importance of the degree of coupling between ice and bed in controlling the amount of basal motion. This coupling is controlled by bed roughness and subglacial water pressure; however, bed roughness is often completely ignored, usually because of difficulties in measuring this quantity (Bennett, 2003; Taylor and others, 2004). In this paper, we investigate bed roughness as a potential control on basal motion over the Slessor Glacier region.

METHODOLOGY

Radio-echo sounding data collection

During the austral summer of 2001/02, an airborne RES campaign was carried out in the upper reaches of Slessor Glacier. From a field camp and fuel depot located at 78°58.60′ S, 7°24.97′ W, five airborne RES sorties, covering a total of ~5000 km, were flown, over a grid measuring 200 × 280 km (Figs 1 and 2).

The British Antarctic Survey (BAS) airborne radar is mounted on a de Havilland DHC-6 Twin Otter aircraft. It is a coherent system, transmitting a modulated pulse with a peak power of 1200 W, at a centre frequency of 150 MHz. Pulses are transmitted through a four-element dipole antenna array mounted under the port wing, and return echoes are received by an identical array mounted under the starboard wing. A constant aircraft speed of 60 m s^{-1} was maintained, giving an effective sampling interval of ~25 m. Two different pulses were transmitted alternately: a standard short pulse of 0.25 μs and a 4 μs chirp pulse that gave greater penetration of thick ice and a higher resolution. Consequently, all subsequent analysis was carried out on the 4 μs pulse, giving a true along-track sampling resolution of ~60–75 m, while the across-track spacing of the radar lines was

*Present address: School of GeoSciences, University of Edinburgh, Grant Institute, West Mains Road, Edinburgh EH9 3JW UK.

https://doi.org/10.3189/172756506781828467 Published online by Cambridge University Press

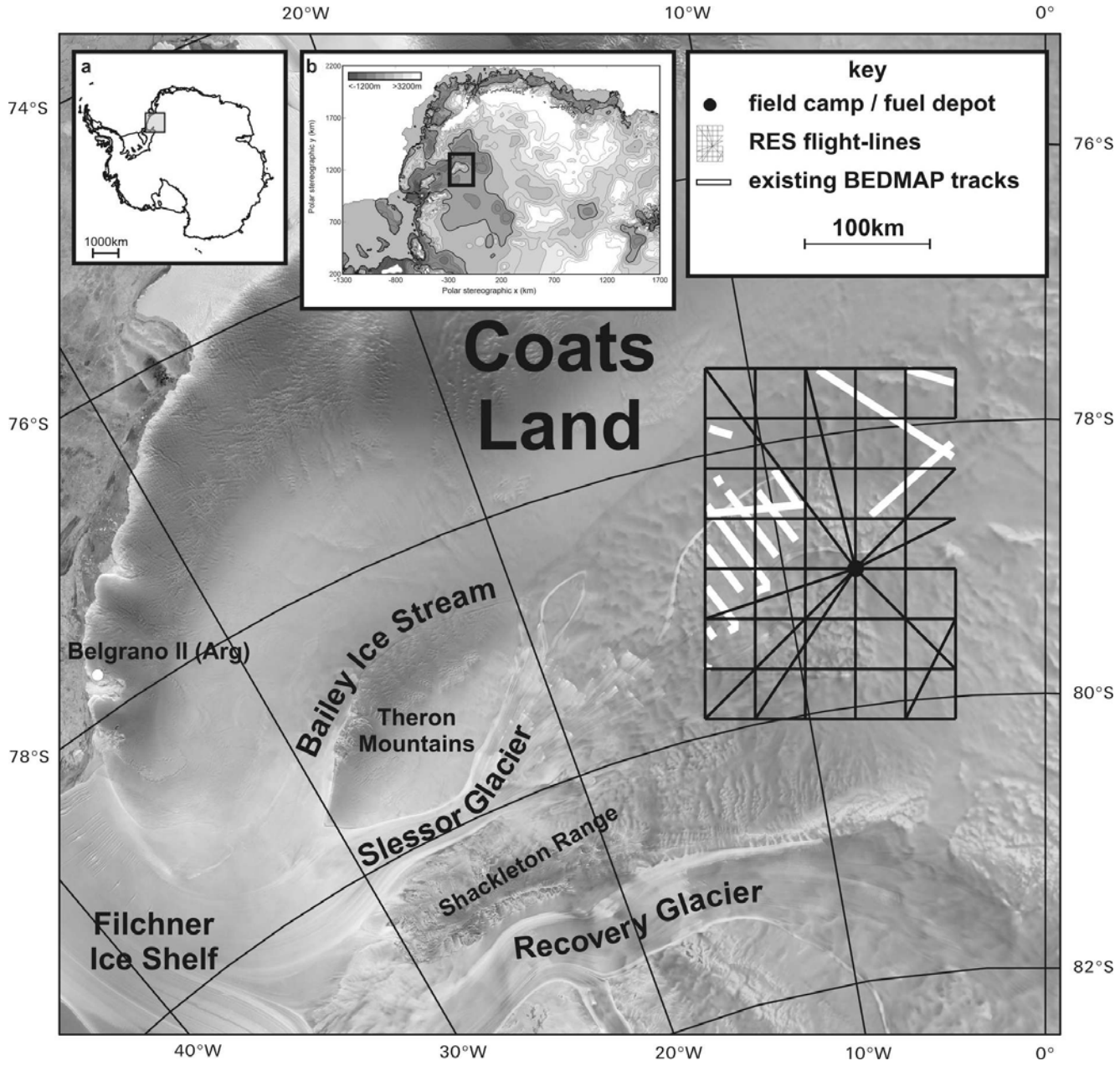

Fig. 1. Part of the RADARSAT Antarctic Mapping Project (RAMP) mosaic of Antarctica (Jezek and RAMP Production Team, 2002), showing the tributaries of Slessor Glacier, with flight-lines and the field camp/fuel depot marked. Inset (a) shows the location of the base map in Antarctica. Inset (b) shows the bed topography for the surrounding region, covering an area of 3000 × 2000 km. The thicker contour marks zero elevation, while the black rectangle delineates the 200 × 280 km region covered by the flight-lines, as shown in the main figure.

40 km. The aircraft's on-board avionics radar system was used to record terrain clearance, which gives a more accurate measure of surface elevation than the RES system itself. Flying was carried out between predefined waypoints (Figs 1 and 2), and coordinates were recorded using an Ashtech GPS (global positioning system) receiver on board the Twin Otter, with reference to a second receiver at the field camp. RES processing was carried out using the seismic processing package ProMAX v2003.0. Data were not migrated, but an automatic gain control (AGC) gain was applied before the locations of the surface and bed were identified using a semi-automatic picking process, and ice thickness was determined as the difference between surface and bed elevation. GPS data were processed using the Trimble package GPSurvey. These procedures are explained in more detail by Rippin and others (2003a).

Roughness measurements

Roughness is a measure of the degree of irregularity of a surface, and was investigated using three different analyses of the radar data:

1. The mean and standard deviation (SD) of bed elevation was determined across the survey area from the raw track measurements of bed elevation. This was done by dividing the area into 5 × 5 km gridcells, and determining the SD within each gridcell (i.e. from all ice-thickness measurements which fall in each cell). Due to the wide across-track spacing of flight-lines (40 km), this measure is effectively an indication of the SD along flight-lines only, apart from at locations where flight-lines cross. Although a single ice-thickness measurement at a point is, in fact, a mean measure of all reflections from

https://doi.org/10.3189/172756506781828467 Published online by Cambridge University Press

within the Fresnel zone (radius 414 m), the measurement is taken to be representative of ice thickness at the nadir. Consequently, this method is considered to give an indication of the variation in bed elevation (and thus our simplest interpretation of roughness) at the resolution of the true along-track sampling interval (~60–75 m), averaged over 5 × 5 km (with an along-track bias). This method is referred to as 'SD of bed elevation'.

2. Roughness was determined through an analysis of the variability of a quantity we term the 'corrected basal reflection power' (BRP_{corr}), which is a measure of the amplitude of the basal reflection power, corrected for ice thickness (cf. Gades and others, 2000; Rippin and others, 2004). The maximum returned power amplitude associated with a basal reflection was identified as the maximum amplitude reached in a window of 50 samples (~2 μs), immediately following the first return, as determined within ProMAX (Rippin and others, 2003a). Peak amplitude was then converted to a measurement of basal reflection power (BRP) based on the radar system parameters. To identify BRP variations due to changes in basal conditions, the reduction of RES signal strength (as a consequence of geometric spreading, absorption and reflection) with path length, and the associated effects of ice density, structure, etc. through the ice column, must be accounted for (Bogorodsky and others, 1985). This was done by determining the relationship between ice thickness and BRP in an inter-tributary area where surface velocities are uniformly low and where we consider the bed reflectivity is likely to be uniform. We then used the derived relationship between ice thickness and measured BRP to calculate a theoretical BRP at any given depth, across the whole survey (taking into consideration the mean properties of the ice column). The quantity 'BRP_{corr}' was then determined as the ratio of the measured BRP to the calculated BRP (as in Gades and others, 2000). Changes in BRP_{corr} across the study area are thus largely considered to be due to variations in basal properties, since the effects of ice thickness, and attenuation through the ice column, have been removed (Gades and others, 2000; Rippin and others, 2004). This method is limited by the implicit assumption that ice properties (impurity content, density, etc.) are uniform across the area. Any variation in these properties is not accounted for, but in the absence of any data regarding this variability, we make this assumption and believe it to be acceptable. As in (1), it is assumed that each BRP_{corr} measurement is indicative of bed properties at the nadir, and consequently this method is also considered to give a measure of variability in bed properties at the ~60–75 m scale, averaged over 5 × 5 km gridcells (again, with an along-track bias). However, in addition to indicating roughness in the traditional sense, this method will reveal patterns in the degree of variability in other bed properties (e.g. sediment distribution, the presence of water and anything else that might effect basal power returns). This indicator of roughness is referred to as 'SD of BRP_{corr}'.

3. It has been shown previously that bed roughness has an impact on the length of the echo in RES reflections (Harrison, 1972; Oswald, 1975; Miners, 1998). As such, a measure of roughness may also be determined from the pulse length of each returned echo. A *drop-off* point was defined following the peak return associated with the bed echo, by identifying where the return amplitude fell below some background noise level (determined in each case as the mean amplitude of each pulse over a 12 μs period, after any remnants of bed return had diminished). The pulse length was then determined as the time between the first return and the drop-off point. Since a perfectly smooth reflector would result in minimal scattering, and thus an echo of short duration (such as over a subglacial lake), a longer pulse length indicates more scattering, and thus a rougher bed within the Fresnel zone. Since this method does not employ any averaging, a measurement of roughness at a point using this method is capable of indicating roughness obstacles as small as the size of a wavelength of the RES signal (~1.12 m). The degree of scattering may also be a function of the nature of the material at the bed (e.g. bedrock, sediment, water) and so this method may also provide information about the relative distribution of these materials. This method is referred to as 'mean pulse length'.

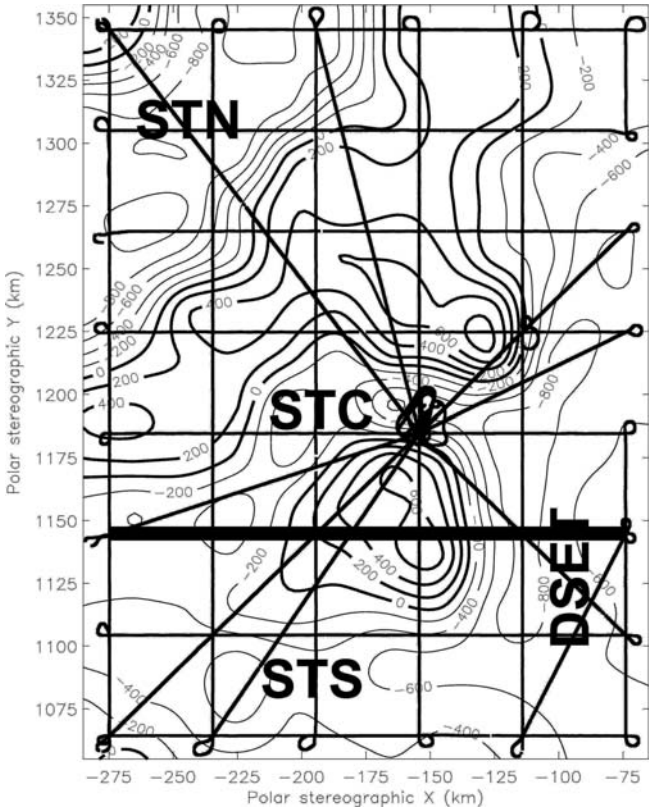

Fig. 2. Contoured bed topography (20 km gridcells) in the survey area, with flight-lines superimposed (in black) to aid orientation in Figure 1. Thicker contours represent elevations (m) above ellipsoid (WGS 84), and thinner contours represent elevations (m) below ellipsoid (from Rippin and others, 2003a). The three troughs containing the tributaries of enhanced flow under investigation – Slessor tributary north (STN), Slessor tributary central (STC) and Slessor tributary south (STS) – and the deep southeastern trough (DSET) are marked. The thicker flight-line is that studied in more detail in Figure 3.

It is important to note that our three methods provide slightly different interpretations of the concept of bed roughness. Method 1 is a measure of raw bed roughness. Method 2 is more a measure of variations in bed properties (not only bed topography, but also the presence or lack of warm ice and

https://doi.org/10.3189/172756506781828467 Published online by Cambridge University Press

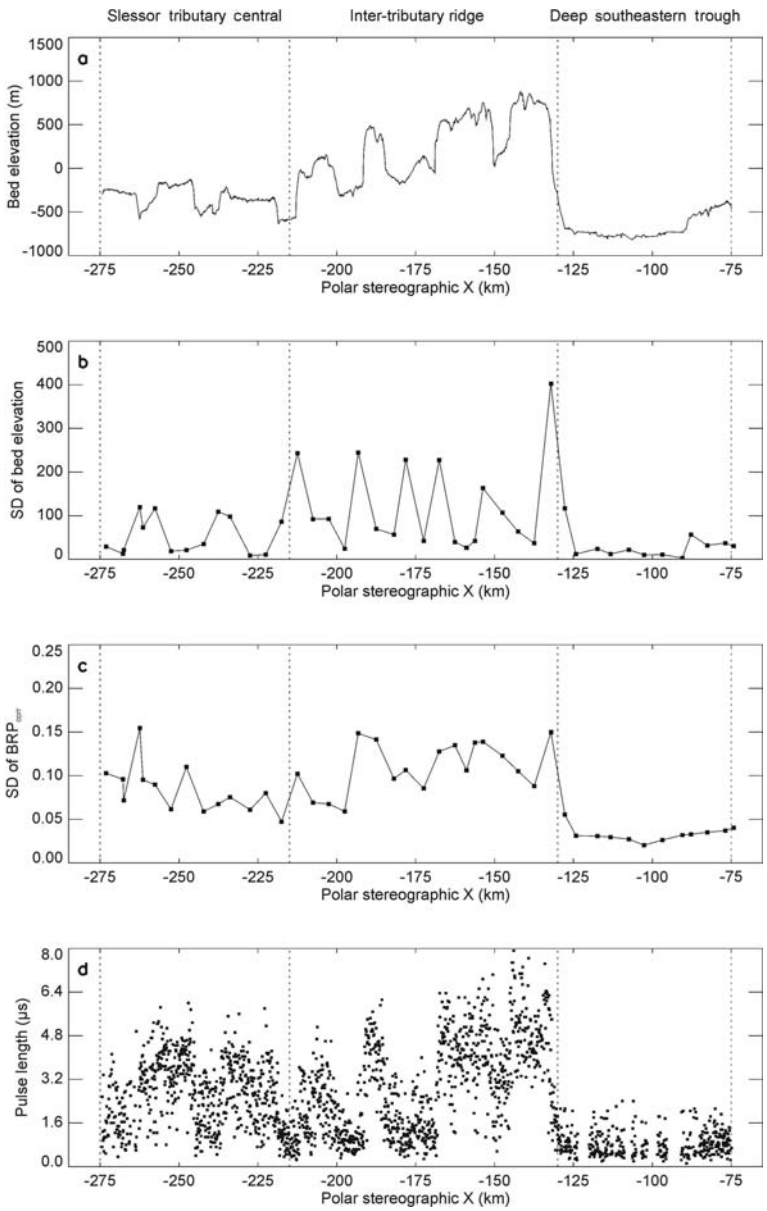

Fig. 3. Example of how the three indicators used as proxies for bed roughness vary along part of one flight-line, which crosses the whole survey area from east to west (approximate *y* coordinates = 1145 km; Fig. 2). (a) Bed topography; (b) SD of bed elevation (~60–75 m resolution, averaged over 5 × 5 km gridcells); (c) SD of BRP_{corr} (~60–75 m resolution, averaged over 5 × 5 km gridcells); and (d) pulse length (μs) (~1.12 m resolution, no averaging).

liquid water, as well as impurities) and may also provide information about the overlying ice column. Method 3 provides a higher-resolution interpretation of raw roughness, but may also contain some information about other bed properties (including bed topography) but is not affected by the overlying ice, since we are isolating the bed reflection. Interpretation of results from all three roughness measurements may provide clues as to the cause of the relative roughness/smoothness.

RESULTS AND ANALYSIS

The area of investigation is divided into a series of subglacial troughs associated with the enhanced-flow tributaries. These are divided from each other by two areas of high bed, which separate the three tributaries of Slessor Glacier. It is important to point out that in our original analyses we referred to the northernmost tributary of Slessor Glacier incorrectly as a tributary of the nearby Bailey Ice Stream (e.g. Rippin and others, 2003a, 2004). More recent inspection of interferometric synthetic aperture radar (InSAR) velocity data clearly indicates that this is, in fact, a tributary of Slessor Glacier (e.g. Bamber and others, 2006). We refer to the three tributaries as: Slessor tributary north (STN), Slessor tributary central (STC) and Slessor tributary south (STS) (Fig. 2).

In addition, there is another large, deep area towards the southeast of the study area. This trough lies upstream of the head of STC and STS, and we refer to this trough as the deep southeastern trough (DSET). We refer to the inter-tributary areas as the Slessor-north/Slessor-central (STN/STC) inter-tributary area and the Slessor-central/Slessor-south (STC/STS) inter-tributary area (Fig. 2).

Prior to our surveys, the data coverage in this region was very limited (note the sparse existing BEDMAP tracks on Fig. 1). There are, however, some existing data from the surrounding wider vicinity, and the bed topography derived

https://doi.org/10.3189/172756506781828467 Published online by Cambridge University Press

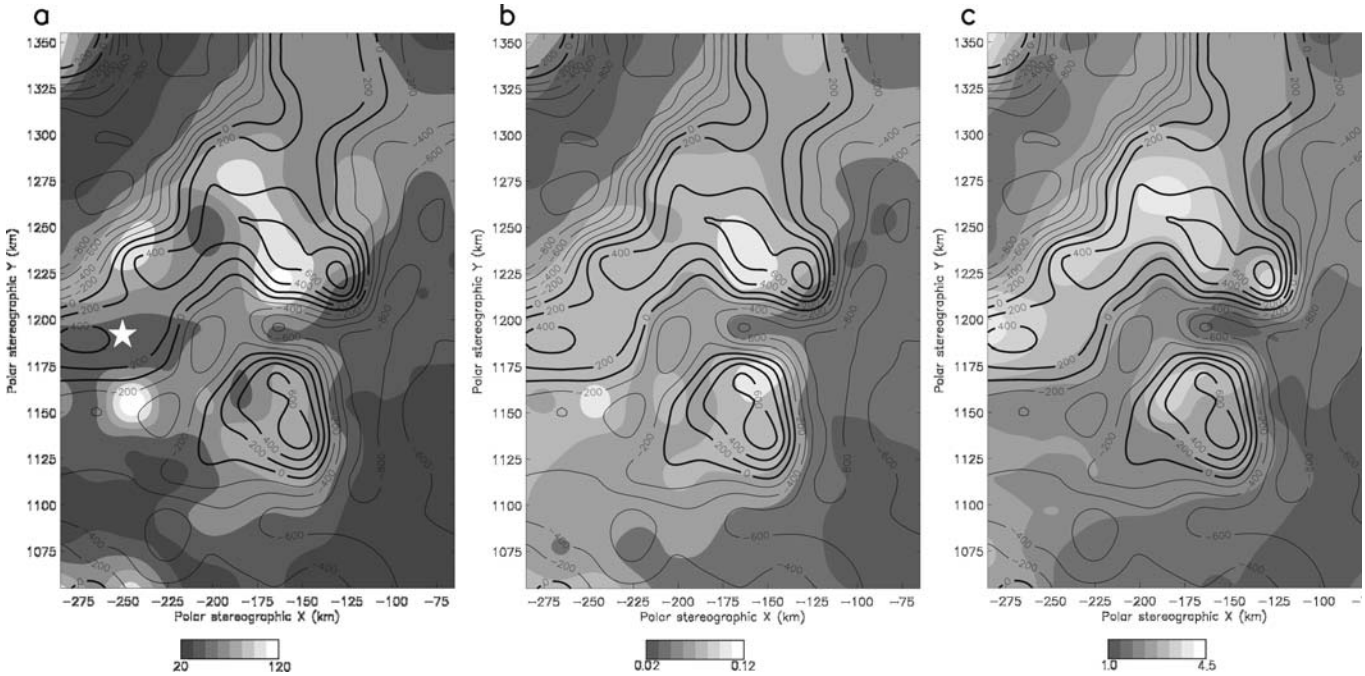

Fig. 4. Three different indicators of roughness over the Slessor region. (a) SD of variation in bed elevation (~60–75 m resolution, averaged over 5 × 5 km gridcells). (b) SD of variation in BRP_{corr} (~60–75 m resolution, averaged over 5 × 5 km gridcells). (c) Pulse length (~1.12 m resolution, no averaging). In all three images, the relevant measure of roughness is contoured and displayed with greyscale shading (darker areas are smoother and lighter areas rougher). In addition, contoured bed topography (m) is also displayed with a 20 × 20 km grid size. As in Figure 2, thicker contour lines indicate elevations above ellipsoid (WGS 84), while thinner contours indicate elevations below ellipsoid. In (a), the star at approximate coordinates (–260,1185) indicates an example of a region of reduced roughness within a slow-moving inter-tributary area, as discussed in the text.

from this portion of the BEDMAP dataset is displayed in Figure 1b. This more extensive coverage reveals that the entire Slessor region lies in a major basin that is largely grounded below sea level under the present ice load, and this submarine grounding persists for some distance (~200–400 km) upstream of the study area.

Figure 3 is an example of how the three indicators of roughness vary along part of one flight-line. The data are from a line which runs approximately east–west across the region, crossing part of the STC trough in the west, an inter-tributary area of high ground in the centre and part of the DSET in the east (see Fig. 2 for location of this line). All three indicators of bed roughness suggest that the DSET is markedly smoother (lower SDs and shorter pulse length) than along the rest of the flight-line. The inter-tributary area is the roughest area according to all three indicators, with STC being marginally smoother. Additionally, the variability of these roughness measures is smallest in the DSET, then STC, and greatest in the inter-tributary area.

These roughness indicators for the whole survey area are shown in Figure 4. We have interpreted our roughness measures across the whole survey area by contouring data using a simple (smoothed) inverse distance interpolation routine (within the data analysis/visualization package IDL v6.3), in which closer raw data points have a greater effect on interpolated points than those further away. The SD of bed elevation indicates that at the scale of the true sampling interval (~60–75 m), there are large areas of rough bed, associated with the areas of high ground (Fig. 4a). These areas constitute slow-moving inter-tributary areas (cf. Fig. 2). There are also substantial areas of bed with much reduced roughness. These areas of reduced roughness are concentrated in STN and the DSET, although there are also areas of reduced roughness along much of STS and in parts of STC, particularly at the down-tributary end (west) (Fig. 4a; cf. Fig. 2). Table 1 quantifies the roughness characteristics of each area by expressing the roughness indicators in each area as a percentage of the mean roughness over the whole region. This table shows that according to the SD of bed elevation indicator, the two inter-tributary areas are significantly rougher than the mean over the whole area (35% and 41% rougher), while the four troughs are relatively smoother (19–68% smoother than the overall mean).

The second indicator of roughness (the SD of BRP_{corr}) suggests that the inter-tributary areas of higher ground are rough (46% and 56% rougher than the overall mean), and that much of STC and STS, although comparatively smoother (4% rougher and 20% smoother than the overall mean, respectively), is still relatively rough compared with the much smoother STN and the DSET (58% and 55% smoother than the overall mean, respectively). The area of reduced roughness in the DSET also extends a short distance into the upper parts of STC and STS, particularly STS (Fig. 4b; Table 1; cf. Fig. 2). These areas of reduced roughness in the upper parts of STC and STS go some way towards accounting for the surprisingly low percentage roughness values (especially in STS) for the troughs as a whole, given that Figure 4b indicates that large parts of these troughs appear significantly rougher.

The roughness revealed by the third indicator (the mean of pulse length) shows a similar pattern (Fig. 4c). The inter-tributary regions are dominated by high roughness measurements, confirmed by the data in Table 1 (64% and 27%

https://doi.org/10.3189/172756506781828467 Published online by Cambridge University Press

Table 1. Roughness characteristics in the four troughs and two inter-tributary areas. In columns two and three, standard deviation (SD) of bed elevation and BRP_{corr}, respectively, are used as proxies for bed roughness, while in column four pulse length is a proxy for roughness. In each case, roughness is expressed as a percentage less than or more than the mean SD, or pulse length, over the whole area. Positive values indicate that the bed is rougher, while negative values indicate that the bed is smoother than the overall mean. Thus, these percentage measurements are relative indicators of roughness

Roughness measure	SD of bed elevation	SD of BRP_{corr}	Mean of pulse length
Resolution	~60–75 m, over 5 × 5 km	~60–75 m, over 5 × 5 km	~1.12 m, at a point
STN	–68.3%	–58.3%	–61.4%
STC	–18.5%	+4.3%	+2.7%
STS	–41.8%	–19.6%	–28.4%
DSET	–67.1%	–54.9%	–62.2%
STN/STC inter-tributary	+34.8%	+46.3%	+63.6%
STC/STS inter-tributary	+41.4%	+56.5%	+27.1%

rougher than the overall mean). By contrast, the deeper trough of STN and the DSET are significantly smoother than elsewhere (61% and 62% smoother than the overall mean respectively; Table 1). STC and STS display an intermediate roughness (3% rougher and 28% smoother than the overall mean; Fig. 4c; Table 1), although, as before, there is an area of reduced roughness that extends from the DSET down the upper part of STS.

We attempted to investigate whether roughness varied both along- and across-flow, in all tributaries, where the orientation of flowlines allowed. These analyses revealed that, using the methods presented here, there was no significant difference in roughness between these two flow directions.

DISCUSSION

STN contains the region's thickest ice (>2800 m; Rippin and others, 2003a) and is characterized by very low roughness according to all three roughness indicators; the magnitude of roughness is similar using all three methods (Fig. 4; Table 1). A smooth bed implies fewer obstacles to sliding, and this may be a result of: (i) erosion of bed obstacles, (ii) infilling of gaps between obstacles by sediment and/or (iii) the presence of basal water which drowns bed obstacles. There are no InSAR velocities available for much of STN, but balance velocities for the region indicate that velocities of >60 m a^{-1} are reached here (Bamber and others, 2006).

Balance velocities were calculated, where the ice sheet is grounded, from surface slope, ice thickness and the mean net surface mass balance, using a two-dimensional finite-difference scheme (Budd and Warner, 1996; Bamber and others, 2000). We are confident of the accuracy of the balance velocities, particularly the location of these tributaries, since errors are relatively small. Surface slope is the most important factor controlling balance velocities, and this is scaled by mass balance (estimated 10% error) and ice thickness (estimated 20% error, although in some locations this is greater because of significant regional variations) (Bamber and Huybrechts, 1996; Vaughan and others, 1999; Bamber and others, 2000). Patterns of tributary flow are not affected by these errors because areas of enhanced flow move at least 100–200% faster than the slower-moving surrounding ice sheet, and errors of a similar order are necessary if thickness is to impact on tributary location (Rippin and others, 2003c). Large-scale modelling experiments carried out by Takeda and others (2002) have indicated that in this region of East Antarctica large parts of the bed reach the pressure-melting point. Additionally, a numerical modelling study has shown that basal motion contributes to a large proportion of flow here (Rippin and others, 2003a). The smooth bed revealed here supports the suggestion that basal motion is important.

Like STN, the DSET contains thick ice (~2800 m; Rippin and others, 2003a) and is also characterized by low roughness according to all three indicators (Fig. 4; Table 1). The roughness magnitudes are very similar to those in STN, but, unlike STN, combined InSAR and balance velocities in much of the DSET are only ~10 m a^{-1} (Bamber and others, 2006), and ice deformation is considered to explain all flow here (Rippin and others, 2003a).

Ice in STC and STS is ~800 m thinner than in STN (Rippin and others, 2003a). InSAR velocities are available (personal communication from I. Joughin, 2002), and indicate that while the eastern, upstream ends of the tributaries reach velocities of ~20 m a^{-1}, at the downstream western end they are >60 m a^{-1} (Bamber and others, 2006). A numerical modelling investigation has indicated that, within the range of uncertainties, virtually all flow within STC and STS may be explained by ice deformation alone, without the need for basal motion (Rippin and others, 2003a). The results presented here generally agree with this observation, although STS is surprisingly smooth (albeit rougher than STN or the DSET). Although ice deformation explains all flow here, perhaps the trough does bear the signature of recent basal motion. Additionally, there is some disagreement as to the roughness of STC at the ~60–75 m scale, derived from roughness methods 1 and 2 (Table 1). This is not of particular concern since, despite the suggestion that these two methods indicate roughness at the same range of scales, we do not expect that identical results would be achieved using both methods, particularly as method 2 may also reflect variations in the overlying ice column.

The two inter-tributary areas between STN and STC, and STC and STS are characterized by slow flow velocities of the order of 5 m a^{-1} and are dominated by internal ice deformation (Bennett, 2003; Rippin and others, 2003a). These inter-tributary areas have rough beds according to all three indicators (Fig. 4; Table 1). There are, however, a small number of regions within the Slessor-north/Slessor-central inter-tributary area which display reduced roughness at the ~60–75 m scale (e.g. Fig. 4a), despite velocities being low.

https://doi.org/10.3189/172756506781828467 Published online by Cambridge University Press

Close inspection of raw track data indicates that these regions consist of small subglacial valleys (not visible in the gridded bed topography because of the small size of these troughs and the 20×20 km grid resolution). It has been shown that relict subglacial valleys may be preserved beneath the East Antarctic ice sheet, where ice velocities are low, as a consequence of cold basal ice (Näslund, 1997). We suggest that in the early stages of ice-sheet growth, when ice cover was much thinner, small valley glaciers may have occupied these troughs, and due to low flow velocities have been preserved. Small regions of smooth bed at the ~60–75 m scale may be a product of these palaeoglaciers.

It should also be noted that in significant areas of STN, there is a loss of radar signal. It is possible that this may be attributed to drastically increased radar absorption, if STN is underlain by temperate ice with a liquid-water layer (Bogorodsky and others, 1985).

Explaining roughness patterns

As stated previously, a smooth bed means fewer obstacles to sliding, either as a consequence of erosion of bed obstacles or the infilling of gaps in a rough bed by water and/or sediment. In an attempt to investigate the feasibility of these proposals and explain the observed patterns of roughness, we investigate two possibilities.

1. Basal water

If basal ice is at the pressure-melting point, water may be present. In order to investigate this, we determined theoretical patterns of glacier-wide subglacial drainage. It is acknowledged that, in general, the detailed structure of the drainage system beneath ice streams and their tributaries is uncertain. While borehole investigations in West Antarctica have indicated that a sheet of water ~2.5 mm thick may be present beneath Kamb Ice Stream, it is uncertain whether this distributed drainage system also links with larger-scale channelized drainage (Kamb, 2001). Regardless of the precise drainage structure, borehole investigations beneath Whillans, Kamb and Bindschadler Ice Streams, Siple Coast, West Antarctica, have indicated that the subglacial drainage system carries substantial amounts of water at a pressure which is approximately equal to the ice overburden pressure (Engelhardt and Kamb, 1997; Kamb, 2001).

We calculate the steady-state subglacial hydraulic potential when subglacial water pressure (P_w) equals ice overburden pressure (P_i). Under such conditions, drainage elements are completely filled with water, and they are orientated at right angles to contours of hydraulic equipotential (e.g. Shreve, 1972). Other workers have investigated the impact of other steady-state drainage scenarios on drainage routing (e.g. when $P_w = 0.5P_i$ or when $P_w = P_a$ (atmospheric pressure); Flowers and Clarke, 1999; Rippin and others, 2003b), but in light of the discussion above, we do not consider these scenarios realistic here.

We have no knowledge regarding flow volumes or specific flow paths, and so the orientation of equipotential contours is used as guidance. Total hydraulic potential (Φ) is the sum of the elevation and pressure potentials and can be expressed as follows (adapted from Shreve, 1972; cf. Rippin and others, 2003b):

$$\Phi = \rho_w g B + [\rho_i g (H - B)],$$

where ρ_w is the density of water (1000 kg m^{-3}), ρ_i is the density of ice (917 kg m^{-3}), g is acceleration due to gravity (9.81 m s^{-2}) and H and B are the elevations of the ice surface and bed respectively (m). Theoretical drainage flows perpendicular to equipotential surfaces, from regions of high to low equipotential (cf. Sharp and others, 1993).

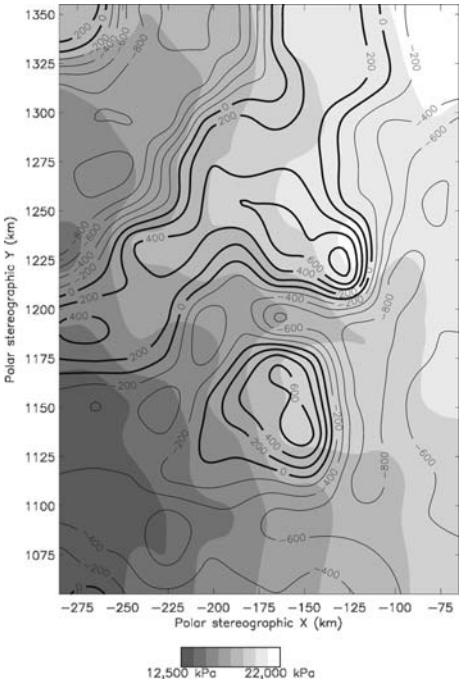

Fig. 5. Contours of hydraulic equipotential (kPa) when $P_w = P_i$. Contours of bed elevation (m) are overlain in black, with thicker contours representing elevations above ellipsoid (WGS 84) and thinner contours representing elevations above ellipsoid, as Figure 2.

Figure 5 shows contours of hydraulic equipotential assuming $P_w = P_i$. These bear some resemblance to contours of surface elevation (Rippin, unpublished data), but the role of subglacial topography is clear to see, with greater potential in the troughs than the inter-tributary regions. Interestingly, potential is greatest in the troughs of STC and STS, but it is clear that any basal water present (assuming everywhere is below the pressure-melting point (Takeda and others, 2002) and water is generated at the bed everywhere across the study region) would be routed at the bed, from the inter-tributary areas, along all three Slessor troughs (perpendicular to equipotential contours) (Fig. 5; cf. Fig. 2). Additionally, there appears to be significant potential drainage from the DSET, westwards into the STC and STS troughs, while the STN trough is comparatively isolated.

This result indicates that any water generated at the bed is likely to be routed to the troughs of STN, STC and STS, and thus we cannot easily invoke the presence of large amounts of liquid water as the cause of the difference in bed roughness between these troughs.

2. Marine sediments

In addition to possible drainage routing, we investigated the potential distribution of marine sediments to explain patterns of roughness. Previous maps of isostatic rebound indicate that the Slessor region was not grounded below sea level in preglacial times, and thus marine sediments, as in most of East Antarctica, cannot be present at the bed (Drewry, 1983). However, previously available ice-thickness data in the

https://doi.org/10.3189/172756506781828467 Published online by Cambridge University Press

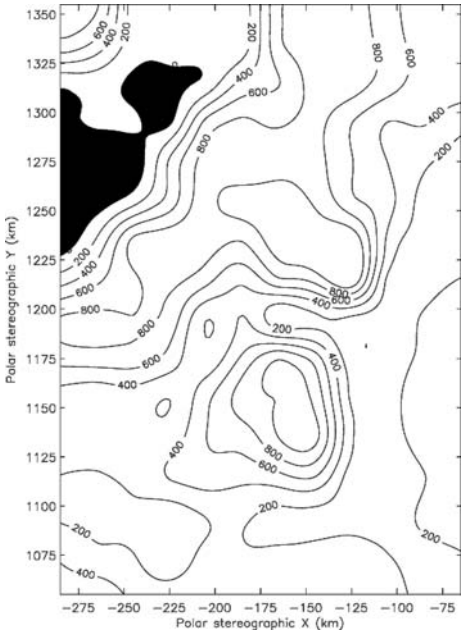

Fig. 6. Subglacial topographic map of the Slessor region, following isostatic recovery as a consequence of the removal of the Antarctic ice load. Contours are in metres above sea level (m a.s.l.), and take account of a 70 m sea-level rise (Hughes, 1998). The shaded area indicates where the bed would have been below sea level in pre-glacial times.

region were of very limited extent (Steinhage and others, 1999; Lythe and others, 2001), and our new maps of bed topography and ice thickness provide data where previous coverage was extremely poor or non-existent. As a result, we use our new data to recalculate isostatic recovery, using a simple Airy compensation which ignores crustal flexure and assumes that all loading of the crust is entirely supported by the asthenosphere. In this model, the unloaded bed elevation following removal of the ice sheet is determined simply from: uplift = ice thickness × [density of ice (917 kg m^{-3})/density of the asthenosphere (3300 kg m^{-3})] (Brotchie and Silvester, 1969; Bamber and others, 2001). This represents a conservative approach to calculating uplift, since it ignores crustal flexure.

Figure 6 shows a new map of isostatically rebounded topography in the region, following the removal of the Antarctic ice load, taking into consideration an estimated 70 m sea-level rise as a consequence of the melting of this ice load (Hughes, 1998). This figure illustrates that while most of the area would have been above sea level in pre-glacial times, there is a substantial region within STN which may have been below sea level (cf. Fig. 2). The possibility that, contrary to generally held opinion, a substantial thickness of marine sediments could have accumulated in STN is of great significance and could be responsible for the proposed basal motion here.

Measurements of total magnetic intensity (TMI) were collected as part of the geophysical survey, and these data provide information about shallow and deep magnetic sources (Bamber and others, 2006). A region of anomalously low value is revealed, coincident with STN, and forward and inverse modelling of these data reveals a non-magnetic sedimentary layer ~3 ± 1 km thick. This sedimentary basin, along with the geographic setting, provides strong evidence that these sediments are of marine origin (cf. Bamber and others, 2006). Additionally, we have calculated driving stresses to be ~50 kPa in STN, which is lower than STC and STS, but very similar to driving stresses calculated for the Siple Coast ice streams which have been shown to lie on marine sediments (Bell and others, 1998; Bindschadler and others, 2001; Blankenship and others, 2001; Rippin and others 2003a; Bamber and others, 2006).

Coupled with the routing of subglacial water beneath STN, the presence of such marine sediments may provide the mechanism by which basal motion might occur, and thus explain a smooth bed. This is because it is now widely accepted that (in West Antarctica) a basal layer of water-saturated dilatant till is required for basal motion to operate (Alley and others, 1986; Blankenship and others, 1986; Studinger and others, 2001).

In the DSET, subglacial water might also exist (Fig. 5), but the bed would not have been below sea level in preglacial times, so marine sediments could not have accumulated here (Fig. 6). The presence of water and low roughness means that the DSET shares a lot of features with STN, implying that it too may have undergone significant basal motion in the past. However, ice deformation rates alone are sufficient to explain current flow rates. We propose that basal motion may have been active here in the past when the East Antarctic interior was thicker and flux rates different. If this is accurate, then any sediment required to form a deformable till layer must have: (1) come from other non-marine sources (e.g. fluvial, lacustrine), (2) been formed in situ by erosion or (3) been transported into the region from elsewhere. This is an important consideration (in all regions, even where we infer the presence of marine sediments) since if East Antarctica has been buried beneath ice for ~36×10^6 years (Ehrmann and Makensen, 1992), then there would have been considerable erosion both here, and upstream in the large subglacial basin in which the Slessor region appears to sit (cf. Fig. 1b). Hallet and others (1996) suggest that 0.1 mm a^{-1} is the minimum erosion rate under temperate glaciers, and 0.01 mm a^{-1} is the minimum for cold-based glaciers (equivalent to total erosion of 3600 m and 360 m, respectively). We are sceptical as to whether such high erosion rates, derived from valley glaciers, are applicable to ice sheets. However, it is possible that there is a deformable till layer present that is a consequence of both in situ erosion and transport of eroded material from upstream.

The rougher bed and lack of basal motion in STC and STS is consistent with them not having an accumulation of sediments (either marine or as a consequence of in situ erosion), even though there are significant drainage routeways along them (Fig. 5a). This, perhaps, serves to indicate the significance of both sediments and water for basal motion to occur.

CONCLUSIONS

In this paper, we have used a new airborne RES dataset to assess bed roughness – an often neglected, but important control on basal motion – in the enhanced flow tributaries of Slessor Glacier. We have also carried out simple modelling of the distribution of subglacial water and possible marine sediments in an attempt to explain the roughness patterns observed. Our analyses enabled us to identify a number of distinct regions:

https://doi.org/10.3189/172756506781828467 Published online by Cambridge University Press

1. Inter-tributary areas where the bed is shallow, velocities low and no basal motion occurs. These are characterized by rough beds, a lack of drainage and any possibility of (marine) sediment accumulation.
2. The fast-flowing STN, where basal motion dominates (Rippin and others, 2003a) and which lies in a deep trough characterized by a smooth bed. Here, marine sediments may have accumulated and subglacial drainage may be present.
3. The moderately fast-moving STC and STS, where all flow can be explained by ice deformation alone (Rippin and others, 2003a). High roughness is evidence of a lack of past basal motion and evidence also of obstacles to current or future basal motion.
4. The DSET, which has a smooth bed but is currently slow-moving. There is no basal motion, despite the necessary conditions for this to occur. We propose that basal motion may have occurred here in the past.

In determining why STN displays such different flow characteristics to the adjacent STC and STS, the degree of bed roughness may be of fundamental importance. It is, however, not clear whether STN has a smooth bed because sediment and water drown bed obstacles, thus enabling basal motion, or if basal motion results in a smoothing of bed obstacles. It is likely that there are feedbacks between bed roughness and the effect on basal motion. It is also important to stress that although we have focused on the presence or absence of marine sediments, it is possible that sediments produced by in situ erosion, as a consequence of basal motion, exist; that sediments exist as a consequence of transport from upstream areas; or that they were deposited under different preglacial scenarios (e.g. lacustrine or fluvial settings).

In assessing the likelihood of areas of bed being above or below sea level, it is important to point out that our model of isostatic recovery is simplistic, and that we have not considered the effects of tectonic elevation change, or the implications of subglacial erosion on bed elevation over the $\sim 36 \times 10^6$ years during which East Antarctica has been buried beneath ice (Ehrmann and Makensen, 1992). However, we believe that identification of part of STN having been below sea level in preglacial times is a significant discovery, and this is backed up by the TMI analyses (Bamber and others, 2006).

Additionally, the role of large-scale bed topography on flow dynamics should not be overlooked, since the deep subglacial valleys where these enhanced-flow tributaries exist are locations where water and sediments collect. Finally, the recognition of adjacent areas of enhanced flow in East Antarctica, with significantly different flow mechanisms, is significant, as is the identification of potential areas of relict enhanced flow, indicating perhaps the ability of these tributaries to 'switch' on and off.

ACKNOWLEDGEMENTS

This work was supported by UK Natural Environment Research Council (NERC) grant GR3/AFI2/65. RES data collection in Antarctica was made possible by the British Antarctic Survey (BAS) Administration and Logistics Division. Particular thanks for assistance in the field are due to D. Leatherdale, P. Jones and P. Woodroffe. Additionally, we are grateful to I. Joughin for providing InSAR velocity data. Finally, we thank the scientific editor, N. Glasser, and three reviewers, M. Truffer, P. Jansson and an anonymous reviewer, who helped to improve this paper considerably.

REFERENCES

Alley, R.B. and I.M. Whillans. 1991. Changes in the West Antarctic ice sheet. *Science,* **254**(5034), 959–963.

Alley, R.B., D.D. Blankenship, C.R. Bentley and S.T. Rooney. 1986. Deformation of till beneath Ice Stream B, West Antarctica. *Nature,* **322**(6074), 57–59.

Bamber, J.L. and P. Huybrechts. 1996. Geometric boundary conditions for modelling the velocity field of the Antarctic ice sheet. *Ann. Glaciol.,* **23**, 364–373.

Bamber, J.L., D.G. Vaughan and I. Joughin. 2000. Widespread complex flow in the interior of the Antarctic ice sheet. *Science,* **287**(5456), 1248–1250.

Bamber, J.L., R.L. Layberry and S.P. Gogineni. 2001. A new ice thickness and bed data set for the Greenland ice sheet. 1. Measurement, data reduction, and errors. *J. Geophys. Res.,* **106**(D24), 33,773–33,780.

Bamber, J.L. *and 6 others*. 2006. East Antarctic ice stream tributary underlain by major sedimentary basin. *Geology,* **34**(1), 33–36.

Bell, R.E. *and 6 others*. 1998. Influence of subglacial geology on the onset of a West Antarctic ice stream from aerogeophysical observations. *Nature,* **394**(6688), 58–62.

Bennett, M.R. 2003. Ice streams as the arteries of an ice sheet: their mechanics, stability and significance. *Earth-Sci. Rev.,* **61**(3–4), 309–339.

Bindschadler, R., J. Bamber and S. Anandakrishnan. 2001. Onset of streaming flow in the Siple Coast region, West Antarctica. *In* Alley, R.B. and R.A. Bindschadler, *eds. The West Antarctic ice sheet: behavior and environment*. Washington, DC, American Geophysical Union, 123–136. (Antarctic Research Series 77.)

Blankenship, D.D., C.R. Bentley, S.T. Rooney and R.B. Alley. 1986. Seismic measurements reveal a saturated porous layer beneath an active Antarctic ice stream. *Nature,* **322**(6074), 54–57.

Blankenship, D.D. *and 9 others*. 2001. Geologic controls on the initiation of rapid basal motion for West Antarctic ice streams: a geophysical perspective including new airborne radar sounding and laser altimetry results. *In* Alley, R.B. and R.A. Bindschadler, *eds. The West Antarctic ice sheet: behavior and environment*. Washington, DC, American Geophysical Union, 105–121. (Antarctic Research Series 77.)

Bogorodsky, V.V., C.R. Bentley and P.E. Gudmandsen. 1985. *Radioglaciology*. Dordrecht, etc., D. Reidel Publishing Co.

Brotchie, J.F. and R. Silvester. 1969. On crustal flexure. *J. Geophys. Res.,* **74**(22), 5240–5252.

Budd, W.F. and R.C. Warner. 1996. A computer scheme for rapid calculations of balance-flux distributions. *Ann. Glaciol.,* **23**, 21–27.

Drewry, D.J. 1983. *Antarctica: glaciological and geophysical folio*. Cambridge, University of Cambridge, Scott Polar Research Institute.

Ehrmann, W.U. and A. Makensen. 1992. Sedimentological evidence for the formation of an East Antarctic ice sheet in Eocene/Oligocene time. *Palaeogeogr., Palaeoclimatol., Palaeoecol.,* **93**(1–2), 85–112.

Engelhardt, H. and B. Kamb. 1997. Basal hydraulic system of a West Antarctic ice stream: constraints from borehole observations. *J. Glaciol.,* **43**(144), 207–230.

Flowers, G.E. and G.K.C. Clarke. 1999. Surface and bed topography of Trapridge Glacier, Yukon Territory, Canada: digital elevation models and derived hydraulic geometry. *J. Glaciol.,* **45**(149), 165–174.

Gades, A.M., C.F. Raymond, H. Conway and R.W. Jacobel. 2000. Bed properties of Siple Dome and adjacent ice streams, West Antarctica, inferred from radio-echo sounding measurements. *J. Glaciol.,* **46**(152), 88–94.

https://doi.org/10.3189/172756506781828467 Published online by Cambridge University Press

Hallet, B., L.E. Hunter and J. Bogen. 1996. Rates of erosion and sediment evacuation by glaciers: a review of field data and their implications. *Global Planet. Change,* **12**(1–4), 213–235.

Harrison, C.H. 1972. Radio propagation effects in glaciers. (PhD thesis, University of Cambridge.)

Hughes, T.J. 1998. *Ice sheets.* New York, etc., Oxford University Press.

Jezek, K.C. and RAMP Product Team. 2002. *RAMP AMM-1 SAR image mosaic of Antarctica.* Fairbanks, AK, Alaska SAR Facility, in association with the National Snow and Ice Data Center, Boulder, CO.

Joughin, I. *and 7 others*. 1999. Tributaries of West Antarctic ice streams revealed by RADARSAT interferometry. *Science,* **286**(5438), 283–286.

Kamb, B. 2001. Basal zone of the West Antarctic ice streams and its role in lubrication of their rapid motion. *In* Alley, R.B. and R.A. Bindschadler, *eds. The West Antarctic ice sheet: behavior and environment*. Washington, DC, American Geophysical Union, 157–199. (Antarctic Research Series 77.)

Lythe, M.B., D.G. Vaughan and BEDMAP consortium. 2001. BEDMAP: a new ice thickness and subglacial topographic model of Antarctica. *J. Geophys. Res.,* **106**(B6), 11,335–11,351.

Miners, W.D. 1998. Electromagnetic reflections inside ice sheets. (PhD thesis, Open University.)

Näslund, J.O. 1997. Subglacial preservation of valley morphology at Amundsenisen, western Dronning Maud Land, Antarctica. *Earth Surf. Process. Landf.,* **22**(5), 441–455.

Oswald, G.K.A. 1975. Investigation of sub-ice bedrock characteristics by radio-echo sounding. *J. Glaciol.,* **15**(73), 75–87.

Rippin, D.M., J.L. Bamber, M.J. Siegert, D.G. Vaughan and H.F.J. Corr. 2003a. Basal topography and ice flow in the Bailey/Slessor region of East Antarctica. *J. Geophys. Res.,* **108**(F1), 6008. (10.1029/2003JF000039.)

Rippin, D. *and 6 others*. 2003b. Changes in geometry and subglacial drainage of Midre Lovénbreen, Svalbard, determined from digital elevation models. *Earth Surf. Process. Landf.,* **28**(3), 273–298.

Rippin, D.M., M.J. Siegert and J.L. Bamber. 2003c. The englacial stratigraphy of Wilkes Land, East Antarctica, as revealed by internal radio-echo sounding layering, and its relationship with balance velocities. *Ann. Glaciol.,* **36**, 189–196.

Rippin, D.M., J.L. Bamber, M.J. Siegert, D.G. Vaughan and H.F.J. Corr. 2004. The role of ice thickness and bed properties on the dynamics of the enhanced-flow tributaries of Bailey Ice Stream and Slessor Glacier, East Antarctica. *Ann. Glaciol.,* **39**, 366–372.

Sharp, M.J. *and 6 others*. 1993. Geometry, bed topography and drainage system structure of the Haut Glacier d'Arolla, Switzerland. *Earth Surf. Process. Landf.,* **18**(6), 557–571.

Shreve, R.L. 1972. Movement of water in glaciers. *J. Glaciol.,* **11**(62), 205–214.

Steinhage, D., U. Nixdorf, U. Meyer and H. Miller. 1999. New maps of the ice thickness and subglacial topography in Dronning Maud Land, Antarctica, determined by means of airborne radio-echo sounding. *Ann. Glaciol.,* **29**, 267–272.

Studinger, M., R.E. Bell, D.D. Blankenship, C.A. Finn, R.A. Arko and D.L. Morse. 2001. Subglacial sediments: a regional geological template for ice flow in West Antarctica. *Geophys. Res. Lett.,* **28**(18), 3493–3496.

Takeda, A., S. Cox and A.J. Payne. 2002. Parallel numerical modelling of the Antarctic ice sheet. *Comput. Geosci.,* **28**, 723–734.

Taylor, J., M.J. Siegert, A.J. Payne and B. Hubbard. 2004. Regional-scale roughness beneath ice masses: measurement and analysis. *Comput. Geosci.,* **30**(8), 899–908.

Vaughan, D.G., J.L. Bamber, M.B. Giovinetto, J. Russell and A.P.R. Cooper. 1999. Reassessment of net surface mass balance in Antarctica. *J. Climate,* **12**(4), 933–946.

MS received 22 December 2005 and accepted in revised form 25 August 2006